IMEKO 22nd TC3, 15th TC5 and 3rd TC22 International Conferences
3 to 5 February, 2014, Cape Town, Republic of South Africa

THE GROWTH OF THE OXIDE LAYER ON SILICON SPHERES AND ITS INFLUENCE ON THEIR MASS STABILITY

M. Borys[1], M. Mecke[2], U. Kuetgens[3], I. Busch[4], M. Krumrey[5], P. Fuchs[6], K. Marti[7], H. Bettin[8]

[1-5,8]Physikalisch-Technische Bundesanstalt PTB, Braunschweig und Berlin, Germany,
[6,7]Eidgenössisches Institut für Metrologie METAS, Bern-Wabern, Switzerland

[1]Michael.Borys@PTB.de, [2]Michael.Mecke@PTB.de, [3]Ulrich.Kuetgens@PTB.de, [4]Ingo.Busch@PTB.de,
[5]Michael.Krumrey@PTB.de, [6]Peter.Fuchs@METAS.ch, [7]Kilian.Marti@METAS.ch, [8]Horst.Bettin@PTB.de

Abstract: The first results of gravimetric measurements of the growth of the oxide layer on single-crystal silicon spheres are presented and compared with a theoretical model and with measurements of the surface layer based on X-ray and ellipsometric methods. From the results, conclusions can be drawn about the quantitative influence of the growth of the oxide layer on the mass stability of silicon spheres.

Keywords: New SI, kilogram, Avogadro project, Si spheres, mass stability, silicon oxide

1. INTRODUCTION

Silicon spheres are used as primary density standards and for the determination of the Avogadro and the Planck constants with the highest accuracy [1, 2]. Therefore, the new definition of the kilogram and its future realisation is currently being prepared by means of silicon spheres [3]. Since not all measurements which are required for these tasks can be performed at the same time and since, after a realisation of a new definition by means of silicon spheres, these spheres will be considered as primary mass standards, knowledge about their mass stability is required for uncertainty analysis, drift corrections and the determination of appropriate realisation intervals. The mass stability of silicon spheres is influenced by the growth of the oxide layer and by the sorption of water and carbonaceous layers on the surface of the spheres. While approved cleaning procedures are applied [4, 5] in order to remove most of the carbonaceous layers and to minimise the amount of physisorbed water, the influence of the growth of the oxide layer on the mass stability of the spheres has not been investigated in detail in the past. From combined X-ray photoelectron spectroscopy (XPS) and ellipsometric measurements performed by Morita et al. [6] on cleaned silicon wafers with (100) orientation it is known that the growth of the oxide layer in air is diffusion limited and follows a logarithmic law. The aim of the investigations described in the following was to measure the growth of the oxide layer over all crystal orientations on quasi-perfect single-crystal spheres made of natural silicon (^{nat}Si) with a nominal mass of 1 kg and to compare the results with the published values given in [6] for silicon wafers with (100) orientation. For this purpose, the growth of the oxide layer on three ^{nat}Si spheres named Sm14, Sm15 and Sm220 was observed with gravimetric, X-ray and ellipsometric measurements.

2. ETCHING OF THE NATIVE OXIDE

The starting conditions of the native oxide growth just after the final chemical-mechanical (CM) polishing step are not known and presumably inhomogeneously distributed over the spheres' surface. Therefore, in accordance with studies about the oxide growth on silicon wafers the spheres were dipped in a 5 % diluted hydrofluoric acid (DHF) etching solution for twenty seconds in order to achieve new and homogeneous starting conditions for native oxide growth [7]. This selective etching removes the existing oxide but does not affect the silicon bulk. Before that, the spheres were treated with an organic solvent cleaning procedure. After the DHF dip, the spheres were bathed in three deionised (DI) water tanks and then placed on a tripod where they were rinsed by some litres of DI water. The silicon surface bonds are known to be terminated by hydrogen and by a very small amount by fluorine after such a procedure. This hydrophobic surface state hinders the growth of the new native oxide for some hours. Hence, this phase was used to dry the spheres in ambient air and to transport them to the mass laboratory where they were stored in ambient air inside the mass comparator. There the native oxide could grow without touching the spheres' surfaces for more than four weeks.

3. GRAVIMETRIC MEASUREMENTS OF THE GROWTH OF THE OXIDE LAYER

The gravimetric measurements were performed on a 1 kg mass comparator (type Sartorius CCL1007) in air under ambient conditions (pressure 1010 hPa, temperature 21 °C, relative humidity 40 %) at PTB. The mass comparator has a weight exchange mechanism with eight positions, a resolution of 0.1 µg and allows mass comparisons with typical standard deviations in air below 0.2 µg. In order to measure the mass increase due to the growth of the oxide layer, a fourth silicon sphere, named PTB02, was used as the mass reference. This sphere was not etched and has been stored over a period of more than six years in ambient air under a

cover. During the measurements, the mass stability was proven to be within ±1 µg by comparison with a secondary stainless steel mass standard. From long-term measurements, it is known that the carbonaceous contamination on a silicon sphere with a nominal mass of 1 kg under laboratory conditions in ambient air amounts to between 1 µg/month and 2 µg/month [4]. Therefore, the mass increase during the measurement time of about one month is considered to be negligible in comparison to the influence of the oxidation process.

In order to be able to compare the gravimetrically measured growth of the oxide layer with the results of X-ray and ellipsometric measurements, the thickness of the oxide layer was calculated from the measured mass increase in due consideration of the surface of the sphere, the stoichiometry and the density of the oxide [8]. During oxidation, only the mass of the oxygen is added to the mass of the sphere, whereas the silicon atoms of the oxide stem from the silicon core of the sphere. Therefore, the mass increase of the sphere is about half of the mass change in the oxide:

$$F_{St} = \frac{2m_O}{m_{Si}+2m_O} = 0.533 \qquad (1)$$

With this result, along with the mass and the density of the sphere and the oxide [8], the oxide-layer thickness can be calculated from the mass gain and vice versa:

$$\frac{\Delta m_{ox}}{\Delta d_{ox}} = \pi d_{sph}^2 \rho_{ox} F_{St} = 32.5\ \mu g/nm \qquad (2)$$

Figure 1 gives a summary of the results of the gravimetrically measured growth of the oxide layers. The observed mass changes of spheres Sm14 and Sm220 are in a good agreement with the logarithmic growth of the oxide layers on the Si wafers described in [6].

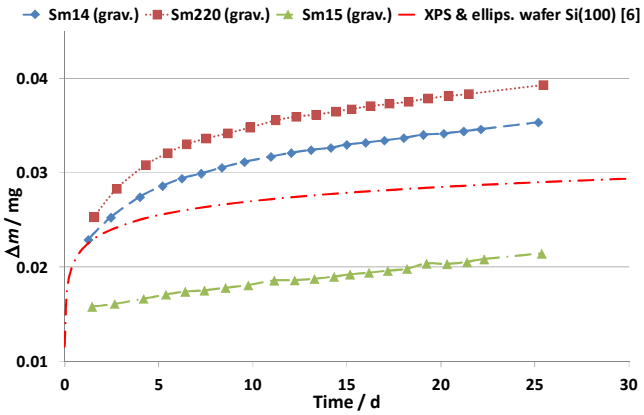

Figure 1. Results of gravimetric measurements of the mass increase of silicon spheres Sm14, Sm15 and Sm220 due to the growth of the oxide layer after etching and comparison with results published in [6] for silicon wafers with (100) orientation. Equation (2) was applied for the conversion of the layer thickness into equivalent mass values.

A significantly smaller and linear growth of the oxide layer was observed on sphere Sm15. Two possible reasons for this different behaviour were identified: Before the etching treatment and the following oxidation, a smaller surface roughness (R_a = 0.5 nm) was measured on sphere Sm15 in comparison with spheres Sm14 (R_a = 2.5 nm) and Sm220 (R_a = 2.4 nm). A second difference was observed with respect to the cleaning state. After completion of the gravimetric measurements, the cleaning state of the spheres was checked by additional cleaning according to the cleaning procedure described in [5]. The observed mass decrease on the surface of Sm15 was about 50 µg and four times higher in comparison with the other spheres. It is therefore assumed that the oxidation process on Sm15 was hindered by an unknown contamination layer on its surface.

In summary, a mass/thickness increase of about 30 µg/0.9 nm, 16 µg/0.5 nm and 34 µg/1.0 nm was observed for spheres Sm14, Sm15 and Sm220 over 25 days after etching.

4. XRR AND XRF MEASUREMENTS

The silicon spheres Sm14, Sm15 and Sm220 were investigated in the PTB laboratory at the synchrotron radiation facility BESSY II in Berlin [9]. The plane grating monochromator beamline was used for the X-ray fluorescence (XRF) analysis of carbon and oxygen, and to access photon energies around the oxygen absorption edge for X-ray reflectometry (XRR) which allows a separation of the oxide layer from a carbonaceous contamination layer [10]. On each sphere, the measurements were performed 50 days and 190 days after etching at the opposite position of two or three marks. For all orientations, the following measurements were performed:

- XRR at several energies around the O-K edge
- XRF mapping scans (121 points on an area of about 1 cm x 1 cm) for oxygen (oxide layer)
- XRF line scans (11 points) for carbon (carbonaceous contamination layer)

Before and after the measurements on the spheres, four flat reference samples with nominal oxide-layer thicknesses between 2 nm and 10 nm were measured by XRR and XRF. The XRR result for the sample with the thickest oxide layer was used to calibrate all XRF measurements. A background correction was applied for the XRF measurements. The XRR measurements on the spheres were evaluated with the same procedure as for the flat samples. For the oxide XRF measurements, also the same calibration factor was used. It was assumed that all oxygen is bound in SiO_2, not e.g. in water, and that the oxide density is constant. The thickness of the oxide layer was measured on two points on the surface of spheres Sm14 and Sm220 and on three points on the surface of sphere Sm15. For this sphere, the difference between the XRR and the local XRF results is always ≤ 0.11 nm. On both other spheres, a slight metallic (mainly copper) contamination has been found in the surface layer, which increases also the uncertainty in XRR. Furthermore, the oxide-layer thickness at both positions on Sm14 differs by about 0.4 nm. The values obtained at the positions marked +, T and D are listed in Table 1. For the reasons given above, only those for Sm15 are suited to investigate the growth of the oxide layer. The XRR measurements at 50 and 190 days after etching are shown in Figure 2.

Table 1. Results of XRR and XRF measurements of the oxide layers at different positions on spheres Sm14, Sm15 and Sm220 (measured mean values with standard uncertainties, $k = 1$).

Sphere	50 days after etching		190 days after etching	
	Thickness XRR / nm	Thickness XRF / nm	Thickness XRR / nm	Thickness XRF / nm
Sm14 +	1.50(23)	1.63(26)	1.60(24)	1.67(25)
Sm14 T	1.21(18)	1.36(20)	1.13(17)	1.40(21)
Sm15 +	0.63(15)	0.71(11)	0.88(15)	0.88(14)
Sm15 T	0.68(15)	0.72(11)	0.94(15)	0.92(15)
Sm15 D	0.65(15)	0.71(11)	0.88(15)	0.88(14)
Sm220 +	0.96(15)	1.16(17)		
Sm220 T	0.98(15)	1.10(17)		

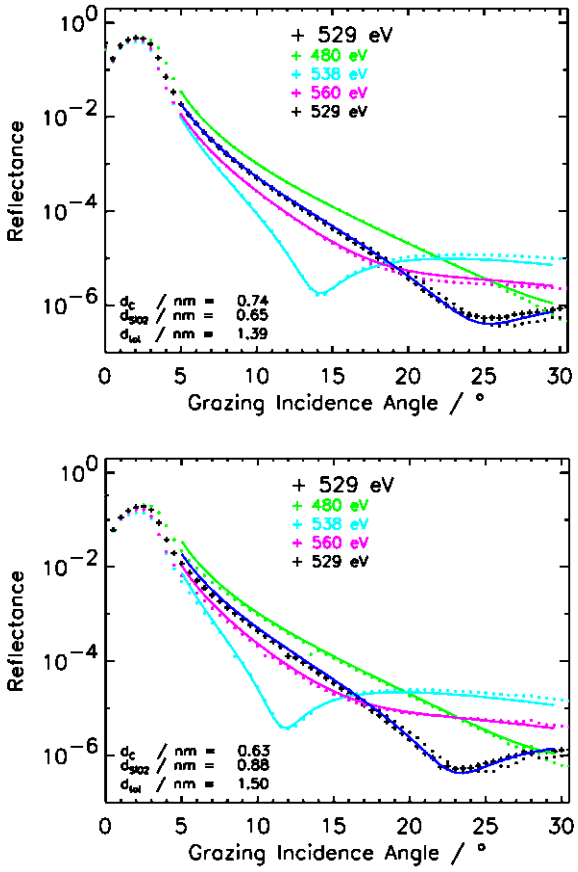

Figure 2: Reflectance of sphere Sm15 at position D, measured 50 (top) and 190 (bottom) days after etching at different photon energies around the oxygen absorption edge. The shift of the minima towards lower angles indicates the growth of the layer thickness.

5. XPS RESULTS

The chemical composition of the surface of the Si spheres was analysed at the mass laboratory of METAS, using a new and unique instrument, which combines high precision mass measurement and element specific surface chemical analysis with X-ray photoelectron spectroscopy XPS [11]. It was especially designed for the analysis of large objects such as real 1 kg standards and artefacts like Si spheres [1, 12].

For the determination of the oxide-layer thickness and the composition, high resolution narrow scan spectra of the Si 2p photoelectron lines were analysed using established procedures [13]. The bulk Si 2p photoelectron line is located at 99 eV binding energy (Figure 3). In the oxidised state, this Si line is shifted to higher binding energies by 2.5 eV for Si_2O_3 and 4.0 eV for SiO_2. This chemical shift enables the identification of quantitatively different oxides. As a result, we found a total oxide-layer thickness of 0.8 nm on spheres Sm14 and Sm15. It consists mainly of SiO_2 (~0.7 nm). In most spectra a very small amount of a submonolayer of Si_2O_3 (~ 0.1 nm) is detectable. As shown earlier [14], this Si_2O_3 is located at the top of the SiO_2 layer. Other oxides are not detectable. The total oxide-layer thickness is much smaller than for native oxidised Si which is (1.5 ± 0.2) nm [12].

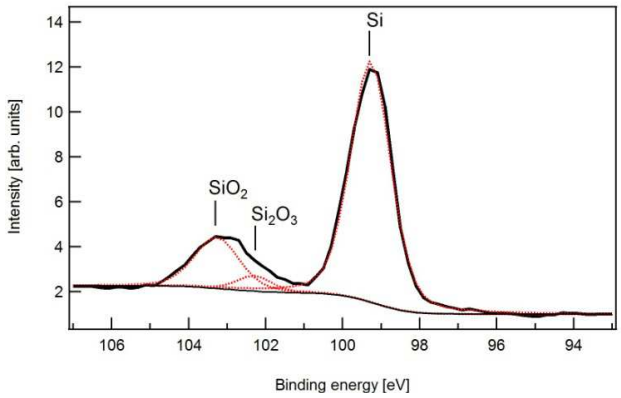

Figure 3. High-resolution scan of the Si (2p) photoelectron line. Due to the oxidation, the Si peaks in SiO_2 and Si_2O_3 are chemically shifted to higher binding energies by 4 eV and 2.5 eV, respectively.

6. MEASUREMENT OF THE OXIDE LAYER TOPOGRAPHY WITH SPECTRAL ELLIPSOMETRY

The spectral ellipsometer of PTB was used to measure the variation of the oxide-layer thickness on the spheres. Spectral ellipsometry (SE) is an optical technique, which gains a very high precision (the related reproducibility is in the order of some ten picometres) with very low time consumption for the measurement (the thickness measurement at a single point is finished within a few seconds). Therefore, the local variation of the oxide-layer thickness is mapped with approximately 5200 measured data points, distributed over the entire surface of the spheres. With these measurements, the so-called thickness topography can be determined and the average oxide-layer thickness calculated. Using calibration points on the spheres with known thickness values from combined XRR/XRF measurements, the average thickness can be determined with a typical standard uncertainty of $u(d_{av}) \approx 0.2$ nm, mainly depending on the local thickness variation at the calibration point.

The results of the ellipsometric measurement of the three spheres are summarised in Table 2. The calibration of the measurement on Sm14 could not be carried out using the calibration point marked with a cross, because of the specific conditions at this calibration point. Therefore, it was decided to apply the standard calibration procedure. To overcome this problem, it was possible to use a second calibration point, marked by a “T”. This calibration point was also covered by ellipsometric measurements in the vicinity

of this point. With an estimation of the thickness value at the calibration point from the local variation of the thickness a rough calibration could be carried out, resulting in an enlarged uncertainty for this sphere.

Already the standard deviation of the measured oxide-layer thickness of the spheres given in Table 2 indicates large differences between the spheres. The small standard deviation of Sm15 indicates a good homogeneity of the native oxide layer on this sphere. The mapping and the histogram (cf. Figures 4 and 5) of this thickness topography underpins the results. As already assumed from the large values of the standard deviation for the Sm14 and Sm220, the mapping of the thickness topography shows a large inhomogeneity of the native oxide layer (cf. Figure 4).

Table 2. Results of the ellipsometric measurement of the thickness topography. The average thickness is the weighted sum of the calibrated ellipsometric thickness values.

Sphere	Average thickness in nm	Standard deviation in nm
Sm14	0.8(7)	0.87
Sm15	0.90(27)	0.38
Sm220	1.35(30)	0.85

The topography gives evidence for a dependency of the oxide growth rate on the crystal orientation at the specific surface area, but the mechanism seems to be different to the well-known effect for a thermal oxide layer. This type of oxide has a small growth rate at (100) surfaces and a high value for (110) of (111) lattice planes [15]. The possible correlation of the thickness variation found in the measurements is the subject of further investigations.

The histograms of Sm14 and Sm220 show a broad peak (compared to Sm15), followed by a shoulder at higher thicknesses.

The ellipsometric mapping of the thickness topography proves the complex nature of the native oxide growth after removing the original oxide layer with an HF dip. Two conclusions can be drawn from these measurements. Firstly, a small number of measurements are not sufficient to calculate the average oxide-layer thickness with the required small uncertainty. Secondly, the growth of a native oxide layer on a bare silicon sphere is not a reproducible process, resulting in a smooth, uniform and stable native oxide layer.

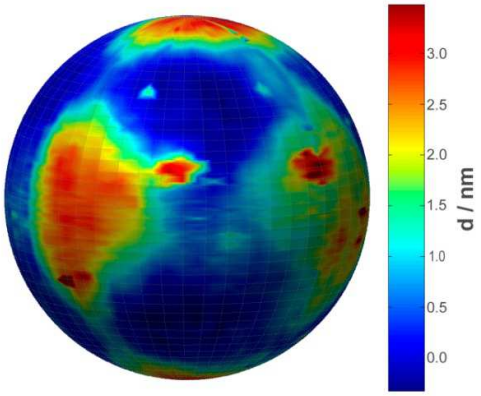

Figure 4. Mapping of the oxide-layer thickness topography of Sm14.

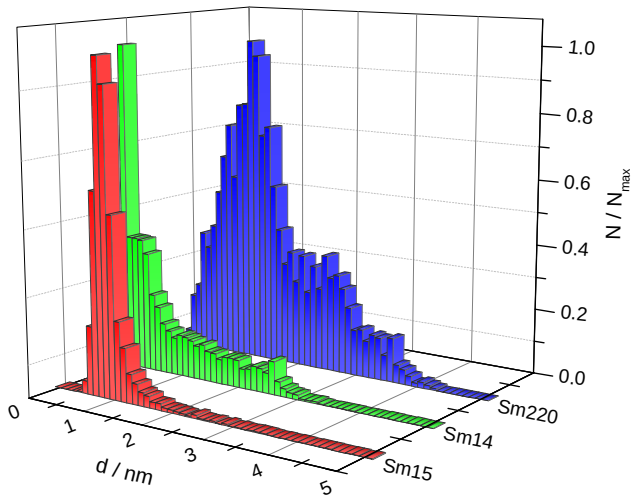

Figure 5. Comparison of the thickness distribution for Sm14, Sm15 and Sm220.

7. SUMMARY OF RESULTS AND CONCLUSIONS FOR MASS STABILITY

The results of gravimetric, XRR, XRF, XPS and SE measurements are summarised and compared with the results published in [6] for silicon wafers with (100) orientation in Figure 6. The uncertainty ranges are given as standard uncertainties ($k = 1$). For the interpretation of Figure 1 it is important to consider that the XRR, XRF and XPS results indicate mean values measured only on two to four points on the surface of the spheres, whereas the gravimetric and the SE measurements represent results with respect to the whole surface of the spheres (see section 6). Although the topography of the oxide layer on spheres Sm14 and Sm220 impaired the calibration of the SE measurements, in general, the results of the X-ray and SE measurements confirm the order of magnitude of the oxide-layer thicknesses determined by extrapolation of the gravimetric results.

The gravimetric results are in good agreement with the characteristic function measured by Morita et al. [6] on cleaned silicon wafers with (100) orientation. The measured mass gain is diffusion limited and follows a logarithmic law. The influence of the oxide layer on the mass stability of silicon spheres can be estimated from this model. According to this model and the results of the gravimetric measurements of spheres Sm14 and Sm220, it can be concluded that their mass increases by about 30 µg to 40 µg in the first two months, 40 µg to 50 µg in the first year, an additional 2 µg to 4 µg in the second year and 1 µg to 2 µg in the third year after etching due to the oxidation process (Table 3). The results reveal that the oxide layer needs a stabilisation time of several months after the etching process before the etched silicon spheres can be used – in combination with an approved cleaning procedure – as high-accuracy mass standards. Further measurements are planned at PTB in order to confirm the results of this first study.

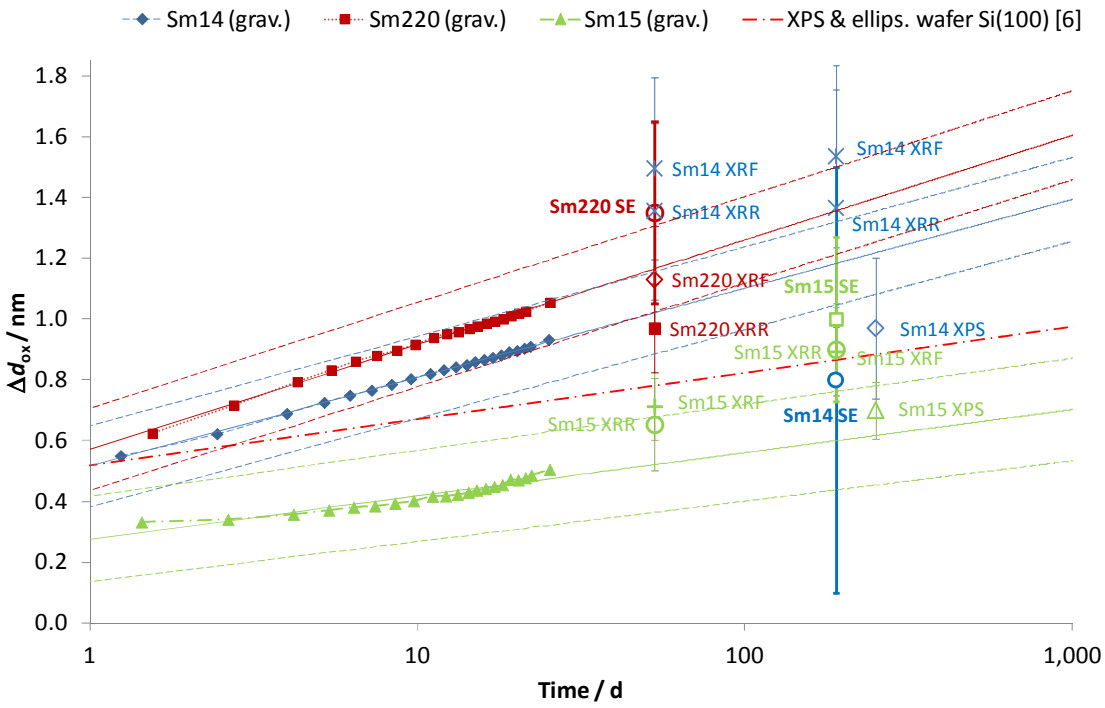

Figure 6: Logarithmic plot of the results of gravimetric, XRR, XRF, XPS and SE measurements of the growth of the oxide layer on silicon spheres Sm14, Sm15 and Sm220 after etching and comparison with results published in [6] for silicon wafers with (100) orientation. Equation (2) was applied for the conversion of the mass gain into an equivalent layer thickness. All X-ray and SE results are given as mean values of the measured points. Dashed lines and uncertainty bars indicate standard uncertainties (k = 1).

Table 3. Estimated influence of the oxidation process on mass stability of silicon spheres Sm14 and Sm220.

Time in days	Sphere Sm14		Sphere Sm220	
	d_{ox} / nm	Δm / µg	d_{ox} / nm	Δm / µg
7	0.76	24.8	0.86	28.1
60	1.04	33.7	1.18	38.5
90	1.09	35.4	1.24	40.5
183	1.18	38.3	1.35	43.9
365	1.27	41.2	1.45	47.3
730	1.35	44.0	1.56	50.7
1095	1.40	45.7	1.62	52.6

ACKNOWLEDGEMENTS

The authors would like to thank all colleagues involved in the manufacture of the spheres in the workshop for ultra-precision machining at PTB.

The work leading to the results described in this publication is part of the European Metrology Research Programme (EMRP), which is jointly funded by the EMRP participating countries within the European Association of National Metrology Institutes (EURAMET) and the European Union.

REFERENCES

[1] B. Andreas et al., “Determination of the Avogadro Constant by Counting the Atoms in a ^{28}Si Crystal”, Phys. Rev. Lett., vol. 106, 030801-1-4, 2011.

[2] P. J. Mohr, B. N. Taylor, D. B. Newell, “CODATA Recommended Values of the Fundamental Physical Constants: 2010”, J. Phys. Chem. Ref. Data, Vol. 41, No. 4, 2012.

[3] http://www.bipm.org/utils/common/pdf/CCM14.pdf

[4] H. Bettin, D. Schiel, M. Vogtmann, H. Niemann, “Cleaning of silicon density standards“, in Proc. XIX IMEKO World Congress, pp. 179-181, 2009.

[5] A. Picard, P. Barat, M. Borys, M. Firlus and S. Mizushima, “State-of-the-art mass determination of ^{28}Si spheres for the Avogadro project”, Metrologia, vol. 48, pp. S112–S119, 2011.

[6] M. Morita, T. Ohmi, E. Hasegawa, M. Kawakami and M. Ohwada, “Growth of native oxide on a silicon surface”, J. Appl. Phys., vol. 68, no. 3, pp. 1272-1281, 1990.

[7] Y. J. Chabal, G. S. Higashi, R. J. Small, “Surface Chemical Composition and Morphology”, in “Handbook of Silicon Wafer Cleaning Technology”, ed. by K.A. Reinhardt and W. Kern: William Andrew, Norwich, pp. 523-618, 2008.

[8] I. Busch, H.-U. Danzebrink, M. Krumrey, M. Borys, H. Bettin, “Oxide layer mass determination at the silicon sphere of the Avogadro project”, IEEE Transaction on Instrumentation and Measurement, vol. 58, pp. 891-896, 2009.

[9] B. Beckhoff, A. Gottwald, R. Klein, M. Krumrey, R. Müller, M. Richter, F. Scholze, R. Thornagel and G. Ulm, “A quarter-century of metrology using synchrotron radiation by

PTB in Berlin", physica status solidi B 246, pp. 1415 – 1434, 2009.

[10] M. Krumrey, G. Gleber, F. Scholze and J. Wernecke, "Synchrotron radiation-based X-ray reflection and scattering techniques for dimensional nanometrology", Meas. Sci. Technol. 22, 094032, 2011.

[11] P. Fuchs, K. Marti and S. Russi, "New instrument for the study of 'the kg, mise en pratique': first results on the correlation between the change in mass and surface chemical state", Metrologia, vol. 49**,** pp. 607-14, 2012.

[12] I. Busch et al., "Surface layer determination for the Si spheres of the Avogadro project", Metrologia, vol. 48, pp. S62-S82, 2011.

[13] M. Seah and S. J. Spencer, "Ultrathin SiO_2 on Si, II Issues in quantification of the oxide thickness", Surf. Interface Anal., vol. 33, pp. 640-652, 2002.

[14] P. Fuchs, "Chemical surface analysis of the test Avogadro sphere PTB-01 investigated by X-Ray Photoemission Spectroscopy XPS", Laboratory Report METAS, 2009.

[15] B. E. Deal, A. S. Grove, "General Relationship for the Thermal Oxidation of Silicon", Journal of Applied Physics 36, No. 12, pp. 3770–3779, 1965.